Study of the Dispersion Characteristics of Planar Chiral Lines

Gonzalo Plaza, Francisco Mesa, *Member, IEEE*, and Manuel Horno, *Member, IEEE*

***Abstract*—This paper analyzes the dispersion characteristics of the fundamental modes of some basic chiral planar transmission lines: microstrip, slot-line, coplanar waveguide (CPW), and a coupled microstrip line, including the possible frequency dependence of the chiral parameters. The dispersion characteristics are computed after finding the zeros of the determinantal equation resulting from the application of the Galerkin method in the spectral domain. Because of the biisotropic nature of the substrate, a 4×4 matrix differential equation has been solved to obtain the spectral dyadic Green's function (SDGF). This function will be explicitly obtained in terms of a closed-form 4×4 transition matrix that relates the transverse electromagnetic fields at the upper and lower interface of the chiral substrate. This fact is key to developing fast computer codes since it avoids numerical matrix exponentiations. The numerical results have shown that the chiral nature of the substrate basically adds an additional parameter to control the propagation characteristics of the analyzed lines and, in general, makes the lines more dispersive, showing even resonant-like behavior.**

***Index Terms*— Chiral media, Galerkin method, planar transmission lines, spectral domain.**

I. Introduction

IN RECENT years, the possibility of manufacturing biisotropic reciprocal materials (generally known as chiral media) at microwave and millimetric frequencies has raised a great theoretical and technological interest. As is well known, chiral composites can be made by embedding chiral microstructures in a low-loss dielectric host medium [1]. The specific electromagnetic properties of chiral materials, which imply an additional cross coupling in the constitutive relations, promisingly extend the possibilities of the isotropic media for designing microwave devices [1]. Thus, numerous applications have been proposed using chiral media, including:

1) antireflection coatings;
2) high-reflection coatings;
3) rotating polarization devices;
4) low reflection antenna radomes; etc.

Recently, a new class of artificial chiral materials suitable for microwave waveguides in planar technology was proposed in [2]. These new media are based on the inclusion of small magnetostatic-wave resonators with a surface metallization in a host medium and are expected to make chiral planar microwave waveguides and transmission lines real technological devices in the very near future.

The effect of bi–iso/anisotropic media on the guided electromagnetic propagation and antenna has also aroused the interest of many researchers. Thus, a great deal of work on the electromagnetic propagation in waveguides filled with biisotropic/chiral materials has been reported in the literature (e.g., [3]–[8], just to mention a few). The use of chiral media in microstrip antennas has also been considered in [9]–[11]; specifically, the possibility of reducing the losses due to surface-waves radiation in a microstrip antenna using a chiral substrate have been proposed in [9], although this topic has been discussed in [10]. Propagation characteristics of bi–iso/anisotropic transmission lines has also given rise to some interesting works. The dispersion characteristics of the fundamental mode of a microstrip on a chiral substrate are obtained in [12] and [13] and on a layered gyromagnetic and chiral substrate in [14]. In [15] and [16], the authors develop a quasi-TEM analysis of an inhomogeneous bi–iso/anisotropic multiconductor transmission line, extending the well-known telegrapher's equations to these media. More recently, transmission-line models are proposed for hybrid modes in bianisotropic structures in [17].

Similar to other types of planar lines, and provided that the substrates have the proper symmetry, the dispersion characteristics of general bianisotropic layered and multiconductor transmission lines can be studied using techniques based on the well-known spectral-domain analysis (SDA). In this paper, the general procedure shown in [18] is now applied and adapted to study the dispersion characteristics of the fundamental modes of several planar lines with chiral substrates. It should be pointed out that this paper is specifically focused on chiral media, i.e., those reciprocal biisotropic media whose existence is out of controversy—nonreciprocal biisotropic media have neither been found nor manufactured, and the possibility of their existence is currently under discussion in the open literature [19], [20].

Before applying the Galerkin method in the spectral domain, the spectral dyadic Green's function (SDGF) of the structure has to be obtained. The SDGF for a grounded chiral slab has been determined in previous work using circularly polarized potential functions [10], [12]. In this paper, the SDGF will be computed in a different way by solving the Maxwell equations in the chiral layer using the 4×4 matrix differential scheme introduced in [21], which is often applied in different contexts in the literature [22]–[29]. Following this scheme, the 4×4 transition matrix relating the Fourier transform

Manuscript received July 28, 1997; revised January 30, 1998. This work was supported by the DGICYT, Spain, under Project TIC95-0447.

The authors are with the Microwave Group, Department of Electronics and Electromagnetisim, Facultad de Física, Universidad de Sevilla, 41012 Seville, Spain.

Publisher Item Identifier S 0018-9480(98)05504-5.

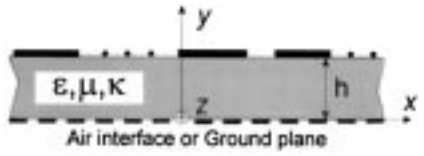

Fig. 1. Generic planar chiral transmission line.

of the transverse electromagnetic fields at the upper and lower interfaces of the layer will be determined. Although the transition matrix of a general bianisotropic layer must be computed numerically as the exponential of a certain 4×4 matrix, in this paper, this matrix will be obtained in closed form for the chiral case. Once the transition matrix is determined, the SDGF is presented in a easy computational form in terms of 2×2 matrices. It is interesting to mention that the transition matrix determined in this paper can also be used to compute the dispersive characteristics of planar chiral layered waveguides following, for instance, the method shown in [8].

Once a fast and accurate method has been developed for computing the propagation constants of general layered chiral lines, the propagation characteristics of a set of different basic printed lines will be analyzed. In the first three numerical examples presented in this paper, some basic lines [microstrip lines, slot-line, and coplanar waveguide (CPW)] will be analyzed, assuming that the constitutive parameters of the chiral substrate are constants over the frequency range of interest. However, this approach would provide good results only if the range of frequencies of interest is taken to be far from any material resonance [1]. Thus, in order to complete this paper, we have included as a final example the study of the dispersion of the fundamental mode of a microstrip also considering a dispersive behavior for the constitutive parameters of the chiral substrate. As an approximate dispersive model for the chiral substrate, we have used the model proposed in [30] for chiral media made by embedding small conducting helices in a lossy isotropic achiral host material.

II. Analysis

In this section, the dispersion characteristics of planar chiral transmission lines will be obtained solving the corresponding integral equation for the surface-current densities/electric fields on the conductors/slots using the Galerkin method in the spectral domain after explicitly obtaining the SDGF.

A. Integral Equation

The cross section of the generic chiral line under study is shown in Fig. 1. In order to make the analysis as general as possible, the specific type of metallizations on the upper interface of the layer and the boundary condition at the lower interface will be specified later for each of the considered lines. Assuming a field dependence of the type $\exp(-jk_z z + j\omega t)$ and homogeneity along the x-direction (see Fig. 1), the transverse components of the electric field $\mathbf{E}_t$ (namely, the components perpendicular to the y-axis) at the upper interface of the layer can be expressed as a function of the surface-current density $\mathbf{J}_s$ by means of the spatial dyadic Green's function $\overline{\mathcal{G}}(x - x', k_z, \omega)$. For the strip-like case, enforcing the transverse electric field to vanish on the strip conductors $\mathbf{E}_t(x) = 0$, the usual integral equation for the surface-current density is expressed as

$$\mathbf{E}_t(x) = \int_{-\infty}^{\infty} \overline{\mathcal{G}}(x - x', k_z, \omega) \cdot \mathbf{J}_s(x') dx' = 0. \quad (1)$$

In the analysis of slot-like lines, the integral equation is posed in terms of the transverse electric field in the slots after enforcing the surface current density to vanish at the slots

$$\mathbf{J}_t(x) = \int_{-\infty}^{\infty} \overline{\mathcal{L}}(x - x', k_z, \omega) \cdot \mathbf{E}_t(x') dx' = 0 \quad (2)$$

where $\overline{\mathcal{L}}(x - x', k_z, \omega)$ operator is the inverse of $\overline{\mathcal{G}}(x - x', k_z, \omega)$.

The above integral equations will be solved making use of spectral-domain techniques, requiring then the computation of the SDGF, $\overline{\mathbf{G}}(k_x, k_z, \omega)$—namely, the Fourier transform in the x-direction of the spatial dyadic Green's function $\overline{\mathcal{G}}(x - x', k_z, \omega)$. In Section II-B, the SDGF will be explicitly obtained for the different boundary conditions which give place to the lines studied in this paper.

B. SDGF

Using the Tellegen notation to describe the constitutive relations in a chiral (biisotropic reciprocal) medium

$$\begin{aligned} \mathbf{D} &= \epsilon \mathbf{E} - jk/c\mathbf{H} \\ \mathbf{B} &= \mu \mathbf{H} + j/c\mathbf{E} \end{aligned} \quad (3)$$

the Maxwell's curl equations for the x-transformed fields in the chiral layer can be written as

$$[\mathcal{R}] \cdot \tilde{\mathbf{E}} = -j\omega\left(\mu\tilde{\mathbf{H}} + j\frac{\kappa}{c}\tilde{\mathbf{E}}\right) \quad (4)$$

$$[\mathcal{R}] \cdot \tilde{\mathbf{H}} = j\omega\left(\epsilon\tilde{\mathbf{E}} - j\frac{\kappa}{c}\tilde{\mathbf{H}}\right) \quad (5)$$

where μ and ϵ are, respectively, the permeability and permittivity of the chiral layer, κ is the dimensionless chirality parameter, c the velocity of light in vacuum, and $[\mathcal{R}]$ the curl operator, which for the assumed field dependence reduces to

$$[\mathcal{R}] = \begin{bmatrix} 0 & jk_z & \dfrac{\partial}{\partial y} \\ -jk_z & 0 & jk_x \\ -\dfrac{\partial}{\partial y} & -jk_x & 0 \end{bmatrix}. \quad (6)$$

After some algebra, the following matrix differential equation is obtained for the transverse electric and magnetic fields:

$$\frac{\partial}{\partial y}\begin{bmatrix} \tilde{\mathbf{E}}_t \\ \tilde{\mathbf{H}}_t \end{bmatrix} = [\mathbf{Q}] \cdot \begin{bmatrix} \tilde{\mathbf{E}}_t \\ \tilde{\mathbf{H}}_t \end{bmatrix}. \quad (7)$$

The expression of the 4×4 $[\mathbf{Q}]$ matrix can be obtained from the general expression corresponding to the bianisotropic case reported, for example, in [8] and [26]. However, it will be shown later that in our problem it is not necessary to obtain the specific expression of matrix $[\mathbf{Q}]$ for computing the

SDGF. If (7) is now solved, the following relation between the transformed transverse electromagnetic field at the upper and lower interfaces of the layer is found:

$$\begin{bmatrix}\tilde{\mathbf{E}}_t\\ \tilde{\mathbf{H}}_t\end{bmatrix}_u = [\mathbf{P}]\cdot\begin{bmatrix}\tilde{\mathbf{E}}_t\\ \tilde{\mathbf{H}}_t\end{bmatrix}_l \tag{8}$$

where the transition matrix $[\mathbf{P}]$ is given by $[\mathbf{P}]=\exp([\mathbf{Q}]h)$ and the subscripts u and l refer to the upper and lower interfaces of the layer, respectively.

A standard mathematical procedure to calculate the exponential of a matrix makes use of the eigenvectors and eigenvalues of the following matrix:

$$[\mathbf{P}]=\exp([\mathbf{Q}]h)=[\mathbf{A}]\cdot[\mathrm{diag}\{\exp(\lambda_i h)\}]\cdot[\mathbf{A}]^{-1} \tag{9}$$

where $[\mathbf{A}]$ is the eigenvector matrix of $[\mathbf{Q}]$ and λ_i its eigenvalues. The key point of this analysis is that, for a chiral layer, the eigenvectors and eigenvalues of the $[\mathbf{Q}]$ matrix can be obtained directly in an easy way. Thus, it will be shown that these eigenvectors are the left- and right-hand circular polarized plane-waves solutions of the wave equation in an unbounded homogeneous source-free chiral medium, namely the Beltrami fields for the homogeneous unbounded source free case [32].

If, for example, a right-hand circular polarized plane wave is considered, its wavenumber is readily found to be $k_R=\omega(\sqrt{\mu\epsilon}+\kappa/c)$ and its electric- and magnetic-intensity fields [31]

$$\mathbf{E}_R(\mathbf{r})=\tilde{\mathbf{E}}_R\exp[-j(k_x x+k_y y+k_z z)] \tag{10}$$

$$\mathbf{H}_R(\mathbf{r})=\frac{-1}{j\eta}\mathbf{E}_R(\mathbf{r}) \tag{11}$$

with $\eta=(\mu/\epsilon)^{1/2}$ and $k_y=\pm\sqrt{k_R^2-k_t^2}$ ($k_t^2=k_x^2+k_z^2$). Now substituting these solutions into the matrix differential equation (7), the following equation is reached:

$$-jk_y\begin{bmatrix}\tilde{\mathbf{E}}_{R,t}\\ \tilde{\mathbf{H}}_{R,t}\end{bmatrix}=[\mathbf{Q}]\cdot\begin{bmatrix}\tilde{\mathbf{E}}_{R,t}\\ \tilde{\mathbf{H}}_{R,t}\end{bmatrix}. \tag{12}$$

According to the above equation, the transverse fields of these plane waves are eigenvectors of the $[\mathbf{Q}]$ matrix and $-jk_y=\pm\sqrt{k_t^2-k_R^2}$ its associated eigenvalues. Similarly, the transverse fields of the left-hand circular polarized plane waves with $k_y=\pm\sqrt{k_L^2-k_t^2}$ (where $k_L=\omega(\sqrt{\mu\epsilon}-k/c)$ is the left-hand wavenumber), will be the two remaining eigenvectors of the $[\mathbf{Q}]$ matrix associated with the eigenvalues $\pm(k_t^2-k_L^2)^{1/2}$.

The right-hand eigenvectors can now be obtained taking into account that $\mathbf{E}_R(\mathbf{r})$ must satisfy the following equation:

$$\nabla\times\mathbf{E}_R=k_R\mathbf{E}_R \tag{13}$$

and considering the right-hand impedance relation (11). The transverse electric fields of the left-hand eigenvalues can be obtained by duality replacing k_R by $-k_L$ and then using the left-hand impedance $j\eta$ to determine the magnetic intensity transverse fields. After some simple algebra to compute the eigenvectors, the following results are obtained:

$$[\mathbf{A}]=\begin{bmatrix}1 & 1 & 1 & 1\\ \Gamma(k_R) & \Gamma(-k_R) & \Gamma(-k_L) & \Gamma(k_L)\\ \dfrac{-1}{j\eta} & \dfrac{-1}{j\eta} & \dfrac{1}{j\eta} & \dfrac{1}{j\eta}\\ \dfrac{-1}{j\eta}\Gamma(k_R) & \dfrac{-1}{j\eta}\Gamma(-k_R) & \dfrac{1}{j\eta}\Gamma(-k_L) & \dfrac{1}{j\eta}\Gamma(k_L)\end{bmatrix} \tag{14}$$

where

$$\Gamma(k_\alpha)=\frac{k_\alpha^2-k_z^2}{k_\alpha\sqrt{k_t^2-k_\alpha^2}-k_x k_z}. \tag{15}$$

Finally, introducing both matrix $[\mathbf{A}]$ and its inverse in (9), the transition matrix can be written as

$$[\mathbf{P}]_{(4\times4)}=\begin{bmatrix}[\mathbf{K}]_R+[\mathbf{K}]_L & -j\eta[\mathbf{K}]_R+j\eta[\mathbf{K}]_L\\ \dfrac{-1}{j\eta}[\mathbf{K}]_R+\dfrac{1}{j\eta}[\mathbf{K}]_L & [\mathbf{K}]_R+[\mathbf{K}]_L\end{bmatrix} \tag{16}$$

where the 2×2 $[\mathbf{K}]_R$ matrix is given in (17), shown at the bottom of the page, where $\gamma_R^2=k_t^2-k_R^2$ and $\gamma_L^2=k_t^2-k_L^2$. As expected, the $[\mathbf{K}]_L$ matrix is found to be the dual expression of the $[\mathbf{K}]_R$ matrix obtained by just replacing k_R by $-k_L$. It is interesting to mention that the 2×2 submatrix $[\mathbf{P}]_{11}([\mathbf{P}]_{22})$ of matrix $[\mathbf{P}]$ in (16) is a dimensionless matrix relating the Fourier transform of the transverse electric (magnetic) field at the upper and lower interface of the chiral layer. Out diagonal submatrix $[\mathbf{P}]_{12}$ ($[\mathbf{P}]_{12}$) is the transverse impedance (admittance) matrix relating the Fourier transform of the transverse electric (magnetic) field at the upper interface to the Fourier transform of the magnetic (electric) field at the lower one.

Once the closed-form expression for the transition matrix has been explicitly obtained, the SDGF is readily built for the transmission lines considered in this paper. Next, two different cases will be analyzed depending on the boundary condition at the lower interface in Fig. 1:

- *Ground Plane:* In this case, the transverse electric field must vanish at the lower interface. Expressing the surface current density as a function of the discontinuity of the transverse magnetic field, the SDGF $\overline{\mathbf{G}}(k_x,k_z,\omega)$ is given by

$$\overline{\mathbf{G}}(k_x,k_z,\omega)=-\{[\mathbf{Y}]-[\mathbf{P}]_{22}\cdot[\mathbf{P}]_{12}^{-1}\}^{-1}\cdot[\mathbf{T}] \tag{18}$$

where matrix $[\mathbf{T}]=\left[\begin{smallmatrix}0 & 1\\ -1 & 0\end{smallmatrix}\right]$ and $[\mathbf{Y}]$ is the free-space admittance matrix for Fourier transform of the transverse fields

$$[\mathbf{Y}]=\frac{1}{\omega\mu_0 k_{y0}}\begin{bmatrix}k_x k_z & k_0^2-k_x^2\\ k_z^2-k_0^2 & -k_z k_x\end{bmatrix} \tag{19}$$

$$[\mathbf{K}]_R=\frac{\cosh(\gamma_R h)}{2k_R\gamma_R}\times\begin{bmatrix}k_R\gamma_R-k_x k_z\tanh(\gamma_R h) & -(k_R^2-k_x^2)\tanh(\gamma_R h)\\ (k_R^2-k_z^2)\tanh(\gamma_R h) & k_R\gamma_R+k_x k_z\tanh(\gamma_R h)\end{bmatrix} \tag{17}$$

with $k_0 = \omega\sqrt{\mu_0\epsilon_0}$ and $k_{y0}^2 = k_0^2 - k_t^2$ (the sign of k_{y0} has to be chosen for the radiation condition to be fulfilled).

- *Air Interface:* Using the above free-space transverse admittance dyad, the following expression is found for the SDGF:

$$\overline{\mathbf{G}}(k_x, k_z, \omega) = -\{[\mathbf{Y}] - ([\mathbf{P}]_{21} - [\mathbf{P}]_{22}\cdot[\mathbf{Y}]) \cdot ([\mathbf{P}]_{11} - [\mathbf{P}]_{12}\cdot[\mathbf{Y}])^{-1}\}^{-1}\cdot[\mathbf{T}]. \tag{20}$$

The above two SDGF"s [(18), (20)] will now be used as the spectral kernels in the Galerkin procedure.

C. Galerkin Method

Once the SDGF $\overline{\mathbf{G}}(k_x, k_z, \omega)$ has been obtained, (1) or (2) can now be solved in the spectral domain in the usual way [33]. In this paper, the widely used Chebyshev polynomials weighted by the Maxwell distribution will be employed as basis functions to analyze both the strip- and slot-like cases. Thus, in a strip-like structure, the current densities on the ith strip are expanded using the following set of functions:

$$J_{x,n}^i(x) = \frac{4}{\pi w_i}\frac{U_n(\alpha_i)}{n+1}\sqrt{1-\alpha_i^2} \tag{21}$$

$$J_{z,n}^i(x) = \frac{2}{\pi w_i}\frac{T_n(\alpha_i)}{\sqrt{1-\alpha_i^2}} \tag{22}$$

where $T_n(\cdot)$ and $U_n(\cdot)$ are, respectively, the Chebyshev polynomials of the first and second kind, $\alpha_i = (x - x_i)/(w_i/2)$ with x_i being the abscissa of the center of the considered strip and w_i its width. Although the behavior of the current density at the edge of an infinitely thin strip on a chiral substrate differs from that in an isotropic case ($R^{-1/2}$ dependence in the latter case) [34], the proposed basis functions have been checked to provide sufficiently reliable results for the commonly used values of the constitutive parameters. A test of the suitability of the above basis function has been carried out through the convergence of the computed results with respect to the number of basis functions. For all the numerical results presented, it has been found that the convergence is appropriate, i.e., the relative error decreases monotonically as the number of basis functions increases.

After the choice of appropriate basis functions, the standard application of the Galerkin method in the spectral domain leads to posing the dispersion relation of the considered structures in terms of the zeros of the Galerkin determinant. The numerical computation of the integrals appearing in the Galerkin matrix has been sped up, making use of asymptotic techniques as those proposed in [18].

III. Numerical Results

On the basis of the above theory, a Fortran code has been developed to compute the dispersion characteristics of several planar chiral transmission lines. The dispersion characteristics presented in the first three examples have been obtained assuming a constant frequency dependence on the constitutive parameters over the considered range of frequencies. It should then be taken into account that this discussion on these examples is restricted to the application of the above assumption. In a final example, the frequency dependence of the constitutive parameters has been included in the analysis using the model proposed in [30]. Thus, the results corresponding to this final example can be seen as more realistic ones.

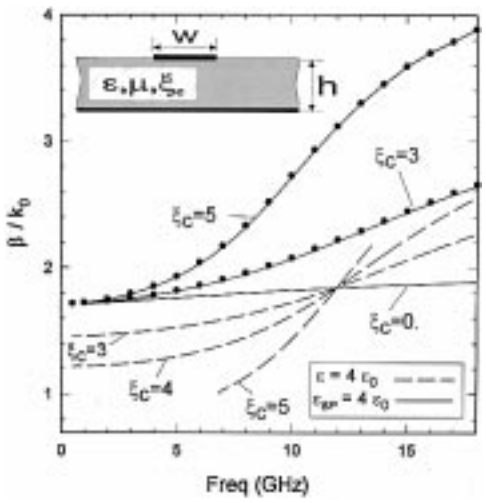

Fig. 2. Dispersion curves of the fundamental mode of a single microstrip on a chiral substrate for different values of the chiral admittance ξ_c (in $10^{-3}\Omega^{-1}$) of the substrate. β/k_0 normalized phase constant. (———): $\epsilon_{\mathrm{BP}} = 4\epsilon_0$ in the Boys–Post system. (– – –): $\epsilon = 4\epsilon_0$ in the Tellegen system. (•): data from [12]. $\mu = \mu_0$ in all cases. Dimensions: $w = h = 3$ mm.

As a first example, a single microstrip on a chiral layer is analyzed. This example has two objectives: to make clear the importance of the full specification of the system of constitutive parameters used to describe the chiral medium, and to check this method and codes by comparing our results with those previously reported in [12] before showing novel results for other lines. The dispersion relation of the fundamental mode of a chiral microstrip is shown in Fig. 2 with two different sets of curves. The first set (solid lines) has been computed in this paper using different values of the chiral admittance $\xi_c = \kappa/(c\mu)$, in the Boys–Post system of constitutive parameters, and keeping both ϵ_{BP} and $\mu_{\mathrm{BP}} = \mu$ constant (subscript BP refers to Boys–Post system). The Boys–Post relations in a biisotropic reciprocal medium are

$$\mathbf{D} = \epsilon_{\mathrm{BP}}\mathbf{E} - j\xi_c\mathbf{B}$$
$$\mathbf{H} = \frac{1}{\mu_{\mathrm{BP}}}\mathbf{B} - j\xi_c\mathbf{E}. \tag{23}$$

This same system was used in [12] and the results of this paper are reproduced in Fig. 2 (dots), showing an excellent agreement with our data. The second set of curves (dotted lines) has been calculated for different values of κ (although, in Fig. 2, the corresponding values of ξ_c have been retained for comparison) and keeping ϵ constant in the Tellegen system. It can be observed that in the first set of curves, the normalized phase constant always increases as the chirality parameter gets higher. The behavior of the second set of curves shows two different zones: low-frequencies zone (in this range of frequencies, the greater the chirality parameter the lesser the phase constant) and high-frequencies zone (in this example, higher than approximately 12 GHz, and the increase of the

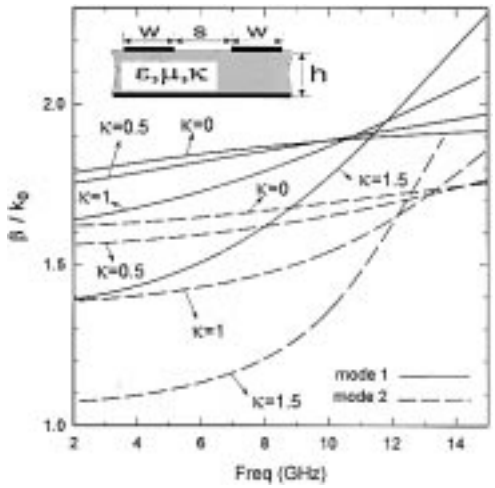

Fig. 3. Dispersion characteristics of the two fundamental modes of a coupled microstrip line on a chiral substrate for several values of the chirality parameter of the substrate. $\epsilon = 4\epsilon_0$, $\mu = \mu_0$. Dimensions: $w = h = 3$ mm and $s = 1.5$ mm.

chirality parameter makes the phase constant grow). It should be noted that the highly dispersive nature of the fundamental mode for high values of the chirality parameter ($\xi_c = 5$) can transform the nature of the fundamental mode from purely propagative to leaky (as β/k_0 is less than the normalized wavenumber of the chiral dielectric slab). This phenomenon would occur for frequencies below 7 GHz for $\xi_c = 5$ and will not be analyzed here since its study is beyond the scope of this paper. It is also interesting to point out that the point at which the chiral curves intersect the nonchiral one is approximately the same. From now on, the Tellegen system of constitutive parameters (3) will be used in the following examples.

As a second example, the dispersion characteristics of the two fundamental modes of a symmetric coupled microstrip line will be studied (see structure in Fig. 3). Specifically, the dependence of the dispersion curves for different values of the chirality parameter is analyzed in Fig. 3. Mode 1 (solid line) refers to the mode that is even for $\kappa = 0$ and mode 2 (dashed line) to the odd mode for $\kappa = 0$. As can be seen in Fig. 3, and similar to the first example, there exist two different ranges of frequencies in the dispersive behavior of both modes. Thus, for low frequencies (less than 10 GHz for mode 1 and less than 12 GHz for mode 2, approximately), the normalized phase constants of both modes decreases as the chirality of the substrate increases. On the contrary, for higher frequencies, the increase of the chirality parameter gives rise to an increase of the phase constants. It can also be observed that two features of Fig. 3 show that the chirality makes the line more dispersive: the difference between the phase constants of modes 1 and 2 (equivalently, between their phase velocities) gets higher as the chirality of the substrate increases, and the slope of the chiral curves always grows as the chirality increases.

After this study, and to complete this example, the current densities on the strips will be studied for both the nonchiral and chiral cases. As is well known, the symmetry shown by the even mode in a symmetric coupled microstrip on an isotropic (nonchiral) substrate can be related to the existence

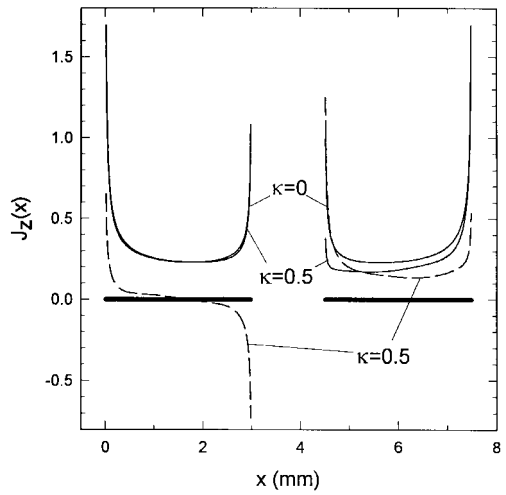

(a)

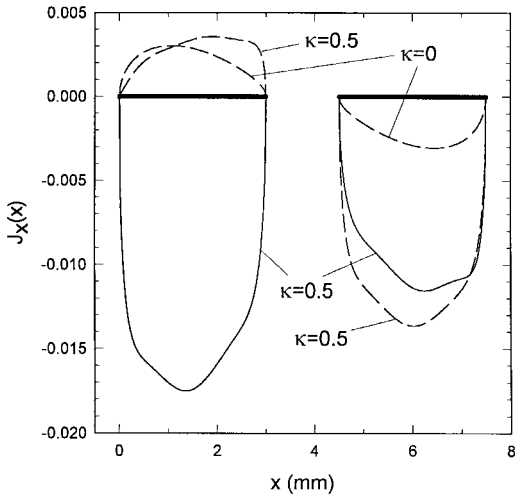

(b)

Fig. 4. Normalized surface current densities on the strip conductors corresponding to mode 1 in Fig. 3 at 5 GHz. (a) Surface-current densities in z-direction. (b) Surface-current densities in x-direction. (———): Real part, (– – –): imaginary part.

of a vertical magnetic wall between the strips (or equivalently, the fields in the left-hand side of the wall are the mirror image of the fields in the right-hand side). The above feature is possible since the constitutive parameters are scalar; namely, they are reflected without changing its sign in a mirror. This means that if Maxwell's curl equations are supposed to be fulfilled in one side of the mirror, then the image fields also fulfill Maxwell's equation without changing the sign in the constitutive parameters. On the contrary, if the substrate is a chiral material, the pseudoscalar nature of κ (which relates polar vectors to axial vectors) requires to change the sign of κ for the mirror image fields to verify Maxwell's curls equations. Clearly, the above situation is impossible if the substrate is homogenous since κ would have the same sign in both sides of the magnetic wall and consequently even modes could not exist in a chiral line. A similar rationale can also be applied to justify the nonexistence of odd modes in chiral lines. The above lack of symmetry is shown in Fig. 4(a) and (b), where the current densities on the strips for the even mode in the

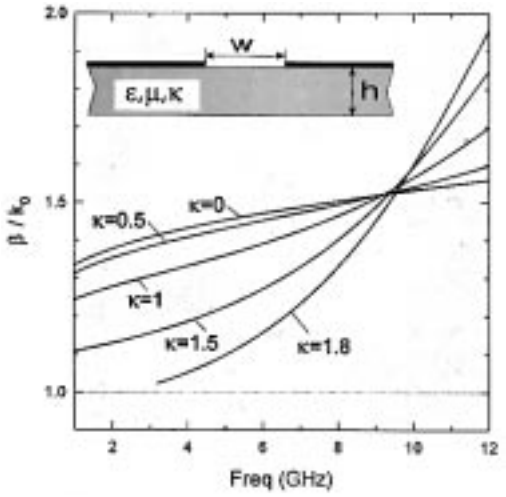

Fig. 5. Dispersion characteristics of the fundamental mode of a chiral slot line for several values of the chirality parameter of the substrate. $\epsilon = 4\epsilon_0$, $\mu = \mu_0$. Dimensions: $w = 1$ mm, $h = 3$ mm.

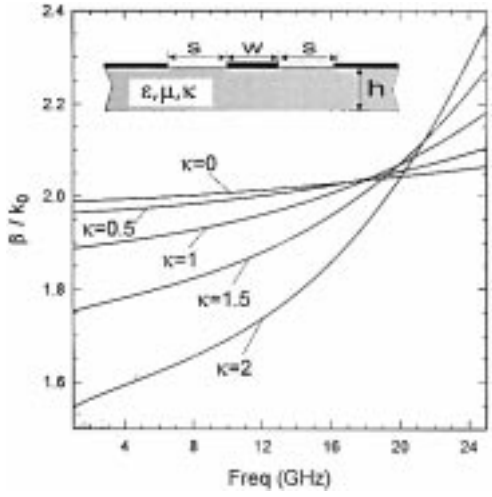

Fig. 6. Dispersion characteristics of the fundamental mode of a chiral CPW for several values of the chirality parameter of the substrate. $\epsilon = 7.35\epsilon_0$, $\mu = \mu_0$. Dimensions: $s = 0.25$ mm, $w = h = 1$ mm.

nonchiral case have been plotted together with the current densities corresponding to the chiral case. Fig. 4(a) shows the break of symmetry for the real part of $J_z(x)$ when $\kappa = 0.5$ and the appearance of an additional nonsymmetric imaginary part. A similar break of symmetry can also be observed for the imaginary part of $J_x(x)$ in Fig. 4(b) together with the appearance of a nonsymmetric real part. In both Fig. 4(a) and (b), the current densities have been normalized, taking the coefficient of the basis function $J^1_{z,0}(x)$ as one.

As a third example, the dispersion curves of the fundamental mode of a slotline and a CPW have been plotted in Figs. 5 and 6, respectively. Similarly to the previously analyzed microstrip-like lines, there also exist two different frequency zones in the dispersion curves of these lines: low and high frequencies zones with the above qualitative behavior of the normalized phase constant with respect to the chirality. It can also be observed in Figs. 5 and 6 that the transition frequency between the low- and high-frequency zones, (i.e.,

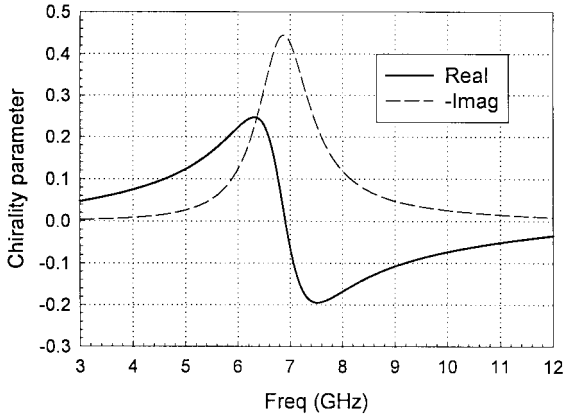

Fig. 7. Dispersive behavior of the chiral parameter following the model proposed in [30] for a chiral material made by embedding helices in a lossy chiral host medium. Host medium: $\epsilon_r = 2.95 - j0.07$, $\mu = \mu_0$. Helices: three-turn helices of cooper-coated wire of 0.1524-mm diameter and surface resistance $R_s = 2.52 \times 10^7 \sqrt{f}$, radius of the 0.625-mm helices and 0.667-mm-pitch.

the frequency at which a chiral dispersion curve intersects the nonchiral dispersion curve) is weakly dependent on the chirality of the substrate. The effect of the chirality on the dispersion behavior is again to make the line more dispersive. This feature can significantly restrict the wide-range frequency applicability of the nonchiral CPW line (see Fig. 6) and could also make the fundamental mode of the slotline become leaky at low frequencies (as happens for $\kappa = 1.8$ in this example).

As a final example, consider the dispersion of the fundamental mode of a microstrip on a dispersive chiral substrate. As is well known, chiral material is always dispersive in practice, with the constitutive parameters showing a strong dependence of the frequency near resonances. In this example, the chiral substrate of the microstrip is an artificial medium made by embedding small conducting helices in a lossy isotropic achiral host material. The dispersive behavior of the effective parameters of this medium are obtained following the model proposed in [30]. This model is a one-resonance model, which includes helix resonance and radiation, near-fields dielectric losses, and coupling effects between helices. Previous to analyzing the microstrip line, the dispersive behavior of the chiral parameter $\kappa(\omega)$ is shown in Fig. 7 for certain characteristics of the helicoidal inclusions and host material. As can be seen, the chiral parameter shows the resonance in this range of frequencies (approximately at 6.9 GHz). Above and below the resonance zone, the chiral parameter shows low losses (imaginary part is almost negligible) and low dispersion (smooth slope in the curves). The dispersion curves for the remaining constitutive parameter (effective permeability and permittivity) of this artificial chiral material also shows a resonance at the same frequency as κ and are reported in [30] in a range from 5 to 10 GHz. Finally, in Fig. 8, the dispersion curve of the microstrip line on this artificial substrate is plotted. As shown in this figure, the behavior of the normalized phase and attenuation constants exhibit a typical anomalous dispersion in the resonance zone qualitatively equal to that corresponding to the constitutive parameters. This same qualitative behavior is expected to be found in the dispersion

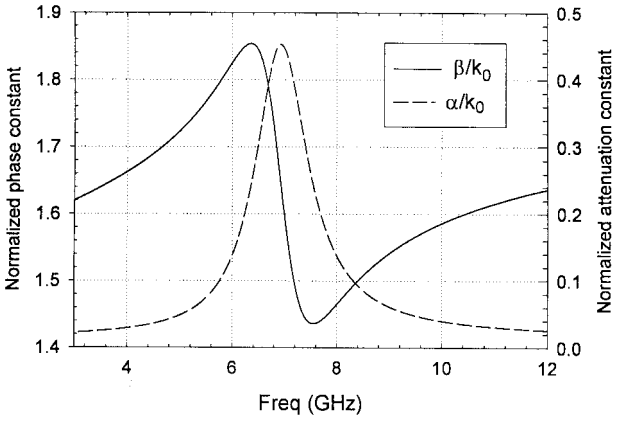

Fig. 8. Normalized phase and attenuation constants corresponding to the fundamental mode of a single microstrip line on the dispersive chiral substrate referred to in Fig. 7. Dimensions: $w = 3$ mm, $h = 10$ mm.

relations of other lines when the frequency dependence of the chiral parameters is taken into account. Due to the presence of high losses at the resonance region, this feature might be advantageously used for the design of reject-band filters.

IV. Concluding Remarks

This paper presents a systematic method to obtain the dispersion characteristics of planar chiral transmission lines. The method employed here can readily take into account any dispersive behavior of the chiral substrate with respect to the frequency and, thus, the application of the method can provide a general view of the main features of the effect of the chirality on the dispersion curves of the fundamental modes in planar chiral transmission lines. This study is relevant in the discussion of possible further technological applications of this type of lines.

The numerical implementation of the method has been carried out by solving the corresponding integral equation using the Galerkin method in the spectral domain. Direct expressions of the SDGF for different boundary conditions have been presented in terms of a closed-form expression of the 4×4 transition matrix of the chiral substrate. The closed-form expression of the transition matrix has been obtained making use of the existence of left- and right-hand circular polarized plane waves propagating in the chiral medium. The use of this closed-form expression has avoided the numerical matrix exponentiations usually performed to compute this matrix, considerably reducing the central processing unit (CPU) time on a computer.

The analyzed examples (single and coupled microstrip lines, slot line, and CPW, assuming the constitutive parameters of the chiral lines as constant in the frequency range) show the existence of a similar dispersive behavior of the fundamental modes in the considered range of the chirality. Specifically, there appear two zones of frequencies in the dispersion curves: low-frequencies range (the greater the chirality the lesser the phase constant), and high-frequencies range (the increase of κ makes the phase constant decrease.) It is interesting to point out that chirality increases the dispersive character of the lines and may even give place to the appearance of low-frequency leakage for the fundamental mode. When the constitutive parameters of the chiral substrate are considered frequency dependent, the resonant-like behavior of the propagation constants of the line has also been shown.

References

[1] H. Cory, "Chiral devices—An overview of canonical problems," *J. Electron. Waves Applicat.*, vol. 9, pp. 805–829, 1995.
[2] E. O. Kamenetskii, "On the technology of making chiral and bianisotropic waveguides for microwave propagation," *Microwave Opt. Technol. Lett.*, vol. 11, pp. 103–107, Feb. 1996.
[3] P. Pelet and N. Engheta, "The theory of chirowaveguides," *IEEE Trans. Antennas Propagat.*, vol. 38, pp. 90–98, Jan. 1990.
[4] C. R. Paiva and A. M. Barbosa, "A linear-operator formalism for the analysis of inhomogeneous biisotropic planar waveguides," *IEEE Trans. Microwave Theory Tech.*, vol. 40, pp. 672–678, Apr. 1992.
[5] I. V. Lindell, "Variational method for the analysis of lossless bi-isotropic (nonreciprocal chiral) waveguides," *IEEE Trans. Microwave Theory Tech.*, vol. 40, pp. 402–405, Feb. 1992.
[6] L. Zhang, Y. Jiao, and C. Liang, "The dominant mode in a parallel-plate chirowaveguide," *IEEE Trans. Microwave Theory Tech.*, vol. 42, pp. 2009–2012, Oct. 1994.
[7] H. Cory and S. Waxman, "Wave propagation along a fully or partially loaded parallel plate chirowaveguide," *Proc. Inst. Elect. Eng.*, vol. 141, pp. 209–306, Aug. 1994.
[8] G. Plaza, F. Mesa, and M. Horno, "Computation of propagation characteristics of chiral layered waveguides," *IEEE Trans. Microwave Theory Tech.*, vol. 45, pp. 519–526, Apr. 1997.
[9] N. Engheta and P. Pelet, "Reduction of surface wave in chirostrip antennas," *Electron. Lett.*, vol. 27, pp. 5–6, Jan. 1991.
[10] D. M. Pozar, "Microstrip antennas and arrays on chiral substrates," *IEEE Trans. Antennas Propagat.*, vol. 40, pp. 1260–1263, Oct. 1992.
[11] A. Toscano and L. Vegni, "A new efficient moment method formulation for design of microstrip antennas over a chiral grounded slab," *J. Electromagn. Waves Applicat.*, vol. 11, pp. 567–592, 1997.
[12] M. S. Kluskens and E. H. Newman, "A microstrip line on a chiral substrate," *IEEE Trans. Microwave Theory Tech.*, vol. 39, pp. 1889–1891, Nov. 1991.
[13] P. K. Koivisto and J. C.-E. Sten, "Quasi-static image method applied to bi-isotropic microstrip geometry," *IEEE Trans. Microwave Theory Tech.*, vol. 43, pp. 169–175, Jan. 1995.
[14] G. W. Hanson, "A numerical formulation of dyadic Green's functions for planar bianisotropic media with application to printed transmission lines," *IEEE Trans. Microwave Theory Tech.*, vol. 44, pp. 144–151, Jan. 1996.
[15] F. Olyslager, E. Laermans, and D. De Zutter, "Rigorous quasi-TEM analysis of multiconductor transmission lines in bi-isotropic media—Part I: Theoretical analysis for general inhomogeneous media and generalization to bianisotropic media," *IEEE Trans. Microwave Theory Tech.*, vol. 43, pp. 1409–1415, July 1995.
[16] ———, "Rigorous quasi-TEM analysis of multiconductor transmission lines in bi-isotropic media—Part II: Numerical solution for layered media," *IEEE Trans. Microwave Theory Tech.*, vol. 43, pp. 1416–1423, July 1995.
[17] F. Olyslager, "Properties of and generalized full-wave transmission lines models for hybrid (bi)(an)isotropic waveguides," *IEEE Trans. Microwave Theory Tech.*, vol. 44, pp. 2064–2075, Nov. 1996.
[18] F. Mesa, R. Marques, and M. Horno, "An efficient numerical spectral domain method to analyze a large class of nonreciprocal planar transmission lines," *IEEE Trans. Microwave Theory Tech.*, vol. 40, pp. 1630–1641, Aug. 1992.
[19] A. Lakhtakia and W. Weiglhofer, "Constraint on linear, spatiotemporally nonlocal, spatiotemporally nonhomogenous constitutive relations," *Int. J. Infrared Millim. Waves*, vol. 17, pp. 1867–1878, 1996.
[20] C. M. Krowne, "Demonstration of marginal nonreciprocity in linear bi-isotropic material and comparison to ferrite material," in *Proc. Bianisotropics'97, Int. Conf. and Workshop Electromagnetics Complex Media*, Glasgow, Scotland, June 1997, pp. 261–264.
[21] D. W. Berreman, "Optics in stratified and anisotropic media: 4×4 matrix formulation," *J. Opt. Soc. Amer.*, vol. 62, no. 4, pp. 502–510, Apr. 1972.
[22] L. B. Felsen and N. Marcuvitz, *Radiation and Scattering of Waves.* Englewood Cliffs: Prentice-Hall, 1973.
[23] C. M. Krowne, "Fourier transformed matrix method of finding propagation characteristics of complex anisotropic layered media," *IEEE Trans. Microwave Theory Tech.*, vol. MTT-32, pp. 1617–1625, Dec. 1984.

[24] W. C. Chew, *Waves and Fields in Inhomogeneous Media.* Piscataway, NJ: IEEE Press, 1995.
[25] F. Mesa, R. Marques, and M. Horno, "A general algorithm for computing the bidimensional spectral Green's dyad in multilayered complex bianisotropic media: The equivalent boundary method," *IEEE Trans. Microwave Theory Tech.,* vol. 39, pp. 1640–1649, Sept. 1991.
[26] J. L. Tsalamengas, "Interaction of electromagnetic waves with general bianisotropic slabs," *IEEE Trans. Microwave Theory Tech.,* vol. 40, pp. 1870–1878, Oct. 1992.
[27] F. Olyslager and D. De Zutter, "Rigorous full-wave analysis of electric and dielectric waveguides embedded in a multilayered bianisotropic medium," *Radio Sci.,* vol. 28, pp. 937–946, Sept./Oct. 1993.
[28] F. Mesa and M. Horno, "Computation of proper and improper modes in multilayered bianistropic waveguides," *IEEE Trans. Microwave Theory Tech.,* vol. 43, pp. 233–235, Jan. 1995.
[29] A. Lakhtakia and W. S. Weiglhofer, "Green function for radiation and propagation in helicoidal bianisotropic mediums," *Proc. Inst. Elect. Eng.* vol. 144, pp. 57–59, Feb. 1997.
[30] A. J. Bahr and K. R. Clausing, "An approximate model for artificial chiral material," *IEEE Trans. Antennas Propagat.,* vol. 42, pp. 1592–1599, 1994.
[31] C. F. Bohren, "Light scattering by an optically active sphere," *Chem. Phys. Lett.,* vol. 29, pp. 458–462, 1974.
[32] A. Lakhtakia, *Beltrami Fields in Chiral Media.* Singapore: World Scientific, 1994.
[33] T. Itoh and R. Mittra, "Spectral-domain approach for calculating the dispersion characteristics of microstrip lines," *IEEE Trans. Microwave Theory Tech.,* vol. MTT-33, pp. 1043–1056, Oct. 1985.
[34] F. Olyslager, "The behavior of electromagnetic fields at edges in bi-isotropic and bi-anisotropic materials," *IEEE Trans. Antennas Propagat.,* vol. 42, pp. 1392–1397, Oct. 1994.

Gonzalo Plaza was born in Cádiz, Spain, on November 26, 1960. He received the Licenciado and Doctor degrees from the University of Seville, Seville, Spain, in 1986 and 1995, respectively, both in physics.

He is currently an Associate Professor in the Department of Applied Physics, University of Seville. His research interest focuses on electromagnetic propagation in planar lines with general bianisotropic materials.

Francisco Mesa (M'94), for photograph and biography, see this issue, p. 1071.

Manuel Horno (M'75) was born in Torre del Campo, Jaén, Spain. He received the Licenciado and Doctor degrees from the University of Seville, Seville, Spain, in 1969 and 1972, respectively, both in physics.

Since October 1969, he has been with the Department of Electronics and Electromagnetism, University of Seville, where he became an Assistant Professor in 1970, Associate Professor in 1975, and Professor in 1986. His main fields of interest include boundary-value problems in electromagnetic theory, wave propagation through anisotropic media, and microwave integrated circuits. He is currently engaged in the analysis of planar transmission lines embedded in anisotropic materials, multiconductor transmission lines, and planar antennas.

Dr. Horno is a member of the Electromagnetism Academy of the Massachusetts Institute of Technology (MIT), Cambridge.